Optical Properties and Electronic Structure of Spinel $ZnRh_2O_4$

D. J. Singh,*,† R. C. Rai,‡ J. L. Musfeldt,‡ S. Auluck,§ Nirpendra Singh,§ P. Khalifah,†,⊥ S. McClure,†,# and D. G. Mandrus†

Materials Science and Technology Division, Oak Ridge, Tennessee 37831, Departments of Chemistry and Physics, University of Tennessee, Knoxville, Tennessee 37996, Physics Department, Indian Institute of Technology, Roorkee, Uttaranchal 247667, India, and Department of Chemistry, University of Massachusetts, Amherst, Massachusetts 01003

Received January 21, 2006. Revised Manuscript Received March 22, 2006

The electronic structure of normal spinel structure $ZnRh_2O_4$ is investigated using combined optical properties measurements and density functional calculations. We find semiconducting behavior with an indirect band gap between crystal field split Rh 4d levels, with a t_{2g} valence band and an e_g conduction band. The band gap is found to be ∼1.2 eV based on a comparison of the calculated and measured optical conductivities. The results are discussed in terms of potential photoelectrochemical applications.

I. Introduction

The 1970s discovery that electrochemical cells with TiO_2 anodes and metal cathodes can decompose water into H_2 and O_2 when exposed to light[1] prompted considerable interest but has yet to lead to a practical solar energy technology.[2,3] The reason is that the band gap of TiO_2 ($E_g \sim 3.2$ eV) is too high to efficiently use the solar spectrum, and materials that are significantly better have not been identified. Specific requirements are a band gap that can effectively use the solar spectrum (i.e., ∼2 eV), chemical stability in a corrosive aqueous environment, and flat band potentials (band edges) that span the water splitting redox potentials. In particular, the last requirement means that the conduction band edge must be above the H^+/H_2 potential, which is approximately 4.4 eV below vacuum. Although the flat band potential is somewhat pH dependent (by ∼0.5 eV going from pH = 2 to pH = 14), this requirement remains very difficult to satisfy in stable oxides with band gaps near 2 eV. This challenge can be rationalized in chemical terms. Many common stable oxides, including TiO_2, have band gaps between occupied O 2p valence bands and unoccupied metal derived conduction bands. TiO_2 is also known to have interesting quadrupolar transitions on the direct forbidden absorption edge.[4]

The position of the O 2p bands in stable oxides is determined mainly by the Mulliken electronegativity of the O ion, which is approximately 3 eV below the H^+/H_2 potential. While it may be possible to chemically control band gaps via the Madelung potential, such tuning also would be expected to destabilize the oxide because the stabilization of O^{2-} ions by the crystalline Coulomb potential is key to the stability of oxides. The apparent alternative is to use metal oxides where the band gap is not of charge-transfer type between O 2p valence bands and metal conduction bands but rather is within the metal states. Then a stable oxide could have a higher valence band maximum and, thus, a sufficiently high flat band potential accompanied by a smaller band gap. For example, one could consider transition metal oxides, where the transition element is in an octahedral crystal field, and one then has a closed t_{2g} shell with six electrons. This approach is schematically illustrated in Figure 1.

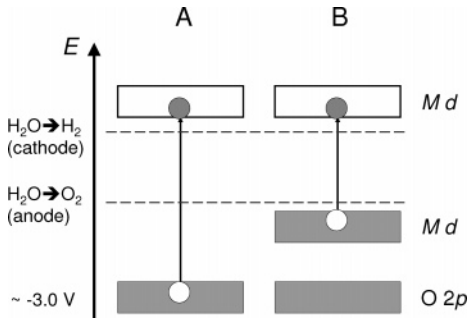

Figure 1. Schematic level schemes for metal oxides in the context of photoelectrochemical hydrogen production. A is the typical case, as in TiO_2. B is the case that may arise in a material with a band gap in the metal d bands, as discussed in the text.

Crystal field splittings in transition metal oxides are mainly the result of hybridization between oxygen 2p levels and metal d states, and the resulting gaps are generally smaller than the 1.5−2.0 eV minimum needed for use in direct photoelectrochemical H_2 production. However, because these gaps originate in hybridization with ligands, it may be that larger values can be obtained in materials with stronger hybridization, especially 4d and 5d oxides. Thus the report by Mizoguchi and co-workers that normal spinel structure $ZnRh_2O_4$ is a p-type semiconductor with a band gap of 2.1

* Corresponding author. E-mail: singhdj@ornl.gov.
† Materials Science and Technology Division, Oak Ridge National Laboratory.
‡ Department of Chemistry, University of Tennessee.
§ Indian Institute of Technology.
⊥ Department of Chemistry, University of Massachusetts.
Department of Physics, University of Tennessee.

(1) Fujishima, A.; Honda, K. *Nature* **1972**, *238*, 37.
(2) Chandra, S. *Photoelectrochemical Solar Cells*; Gordon and Breach, New York, 1985.
(3) Bak, T.; Nowatny, J.; Rekas, M.; Sorell, C. C. *Int. J. Hydrogen Energy* **2002**, *27*, 991.
(4) Pascual, J.; Camassel, J.; Mathieu, H. *Phys. Rev. Lett.* **1977**, *39*, 1490.

10.1021/cm060160v CCC: $33.50
Published on Web 04/27/2006

eV is of considerable interest.[5] Interpretation of photoemission experiments is, however, often complicated by surface sensitivity, especially in three-dimensional oxides. Optical spectroscopy provides a more direct, bulk sensitive measurement. Here we report density functional calculations and optical investigations of the electronic structure, with an eye toward the potential utility of $ZnRh_2O_4$ in photoelectrochemical applications.

II. Methods

$ZnRh_2O_4$ was prepared through the reaction of stoichiometric amounts of ZnO and metallic Rh. A thoroughly ground mixture of the starting materials was pressed into a 1/4 in. pellet and air annealed overnight at incrementally increasing temperatures from 900 °C to 1250 °C. To bring this reaction to completion, multiple heat treatments (∼1 week total) under a flowing oxygen atmosphere at 1175 °C were necessary to fully react the starting materials. Even after this prolonged reaction period a trace amount of Rh (<3%) was visible as minute peaks in the X-ray diffraction pattern.

Near normal reflectance experiments were carried out on a pressed powder sample over a wide energy range (3.7 meV−6.5 eV) using a Bruker 113 V Fourier transform infrared spectrometer and a Perkin-Elmer Lambda 900 grating spectrometer, as described previously.[6] The spectral resolution was 2 cm^{-1} in the far and middle-infrared and 2 nm in the near-infrared, visible, and near-ultraviolet. The optical conductivity and absorption coefficient were calculated by a Kramers−Kronig analysis of the measured reflectance.[7] An open flow cryostat and temperature controller were used for variable temperature measurements.

The density functional calculations were performed using the general potential linearized augmented planewave (LAPW) method,[8,9] at the experimental lattice parameter of 8.506 Å, and the calculated local density approximation (LDA) internal structural parameter u. Two codes were used and cross-checked: a local LAPW code and the WIEN2K code.[10] Local orbitals were employed to treat the high lying semicore states of Rh and the Zn d states and to relax linearization errors. A set of 60 special k points in the irreducible wedge was used for the Brillouin zone sampling during the iteration to self-consistency, and well-converged basis sets of approximately 1500 LAPW functions plus local orbitals were employed. The LAPW sphere radii were 2.1 a_0 for Zn and Rh and 1.6 a_0 for O. The optical calculation was based on 286 k points in the irreducible wedge.

III. Results and Discussion

A. Density Functional Calculations. The LDA band structure is shown in Figure 2. The corresponding electronic density of states and projections onto the LAPW spheres are given in Figure 3. As mentioned, the internal parameter used in the band structure calculations was determined by energy minimization. The calculated value was $u = 0.261\,01$, and the corresponding full symmetry Raman frequency is $\omega = 622\ cm^{-1}$.

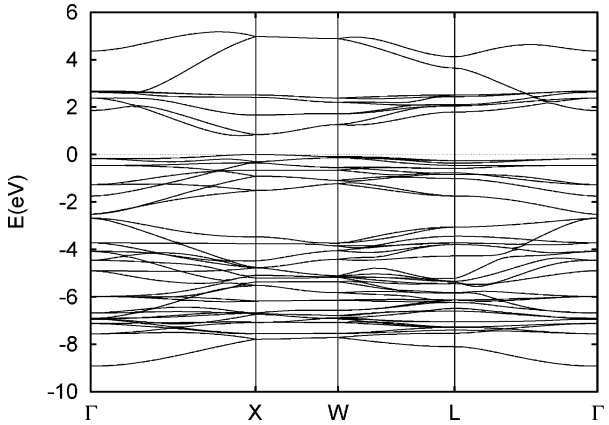

Figure 2. LDA band structure of $ZnRh_2O_4$.

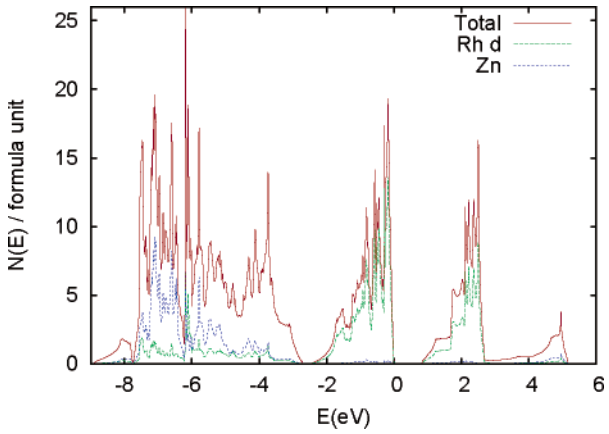

Figure 3. Calculated LDA density of states and projections for $ZnRh_2O_4$. The density of states is on a per formula unit basis, and the projections are onto the LAPW spheres.

The band structure consists of several manifolds. In order of increasing energy these are (1) from ∼−9 eV to ∼−3 eV, O 2p derived bands, (2) from ∼−3 eV to the valence band edge (set to 0 eV), Rh t_{2g} derived bands, and (3) from the conduction band edge to ∼2.5 eV, Rh e_g derived bands and from ∼2 eV to ∼5 eV, Zn s derived bands. Both the Rh t_{2g} and e_g manifolds are narrow. This localization is a characteristic of spinel structure transition metal oxides, AB_2O_4, which have bent B−O−B bonds. Thus, according to the LDA, the band gap is between crystal field split transition Rh 4d manifolds, and the oxygen 2p states are deeper. Thus the basic scenario laid out above for a potentially useful oxide photoelectrode is realized in this compound. However, the LDA band gap is substantially smaller than that required and also much lower than the value estimated in ref 5. The calculated band gap of $E_g(\mathrm{LDA}) = 0.65$ eV is indirect between a valence band maximum at X and a conduction band minimum displaced from X on the $\Gamma-X$ line. The generalized gradient approximation[11] (GGA) band structure is very similar except that the band gap is somewhat larger, $E_g(\mathrm{GGA}) = 0.81$ eV.

Density functional theory has a well-known tendency to substantially underestimate band gaps in most semiconduc-

(5) Mizoguchi, H.; Hirano, M.; Fujitsu, S.; Takeuchi, T.; Ueda, K.; Hosono, H. *Appl. Phys. Lett.* **2002**, *80*, 1207.
(6) Zhu, Z.-T.; Musfeldt, J. L. *Phys. Rev. B* **2002**, *65*, 214519.
(7) Wooten, F. *Optical Properties of Solids*; Academic Press: New York, 1972.
(8) Singh, D. J.; Nordstrom, L. *Planewaves, Pseudopotentials and the LAPW Method*, 2nd ed.; Springer, Berlin, 2006.
(9) Singh, D. *Phys. Rev. B* **1991**, *43*, 6388.
(10) Blaha, P.; Schwarz, K.; Madsen, G. K. H.; Kvasnicka, D.; Luitz, J. *WIEN2K, An Augmented Plane Wave + Local Orbitals Program for Calculating Crystal Properties*; Techn. Universitat Wien: Vienna, 2002.
(11) Perdew, J. P.; Burke, K.; Ernzerhof, M. *Phys. Rev. Lett.* **1996**, *77*, 3865.

tors and insulators. This tendency is due mainly to a discontinuity in the exchange correlation potential and is expected to persist even for the exact density functional. However, Mattheiss[12] argued that because crystal field gaps arise from metal hybridization, which is well-described, and because the character of the valence and conduction band states is essentially the same, these should be better described within density functional theory. If this is correct, then there would still be errors in band gaps, but these would be due to the particular approximate density functional employed. For example, the LDA tends to overestimate hybridization, leading to overestimated exchange interactions, while the GGA has other errors. However, if the argument of Mattheiss holds here, the main error in the gap would be due to the approximate density functional and not the exchange correlation discontinuity. This approach is appealing from a practical point of view because, if correct, density functional band structures could be used as a direct screen for novel oxide photoelectrode materials. However, in that case, the values obtained in the calculation are not consistent with a 2.1 eV experimental (photoemission and inverse photoemission)[5] gap in $ZnRh_2O_4$.

The shape of the LDA density of states is suggestive of a possible resolution to this discrepancy. In particular, the bands at the top of the t_{2g} and e_g manifolds are much less dispersive than the bands at the bottom of the respective manifolds. This shape is characteristic of spinels[13,14] and has been discussed in tight binding terms.[13] The result is an e_g density of states that is small at the bottom of the band and has a prominent peak at higher energy, reminiscent of the basic shape of data of ref 5.

However, optical spectra involve matrix elements, which may be very important here, because the basic $d-d$ character of the transition is dipole forbidden. Thus, hybridization with ligands and the k dispersion may be important. Therefore, we performed calculations of the optical conductivity, based on the band structure, and calculated wave functions using the optical package of the WIEN2K code. As shown in Figure 4, the low energy part of the optical conductivity shows a small onset corresponding to the direct gap followed a more prominent peak at higher energy. This supports the above conjecture about the discrepancy of the previously reported and calculated band gaps.

B. Measured Optical Properties. Figure 5 displays the optical conductivity of $ZnRh_2O_4$ at 5 and 300 K as a function of energy. The spectra show a series of electronic excitations with an ~1.5 eV onset to the conductivity. These results are consistent with previous inverse photoemission studies,[5] with the exception of the low energy electronic structure (discussed below). The shape is similar to that of the LDA calculations, except that the onset is at somewhat higher energy, and the minimum in the LDA conductivity at ~4.1 eV is not evident in the experimental spectrum.[16] Significantly, the peak positions agree well, including the peak near

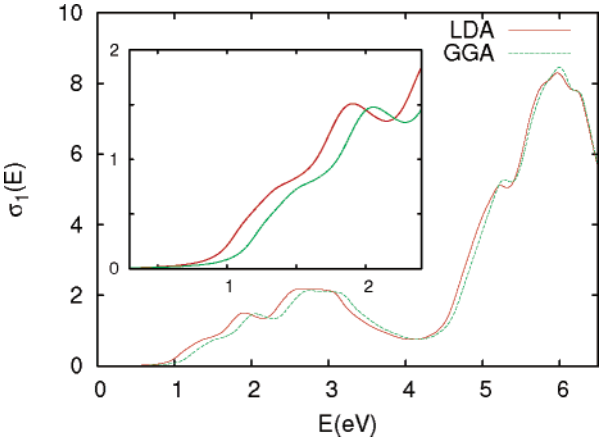

Figure 4. Calculated LDA and GGA optical conductivity of $ZnRh_2O_4$ (arbitrary units), with a 0.1 eV broadening. The inset is a blow-up in the low energy region.

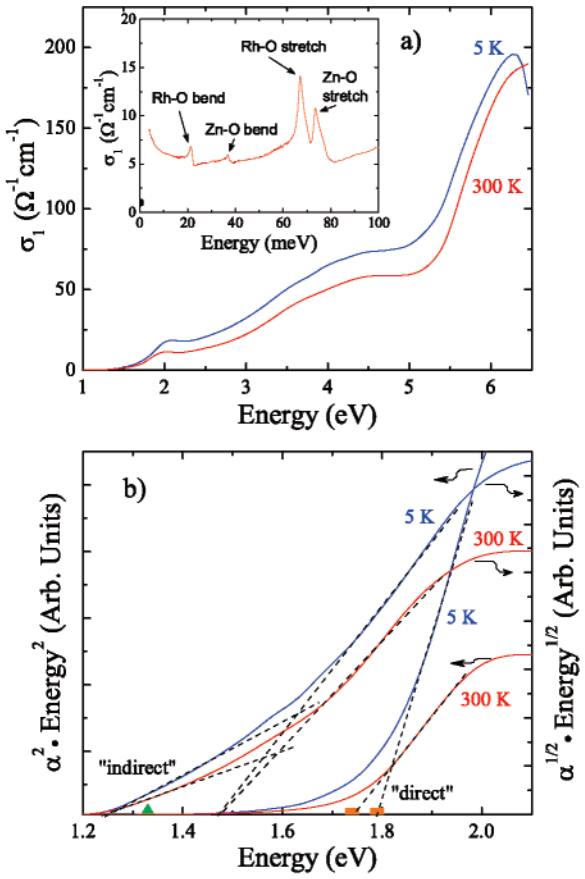

Figure 5. (a) Optical conductivity spectra of $ZnRh_2O_4$ at 5 (blue) and 300 K (red), extracted from the measured reflectance by a Kramers−Kronig analysis. The inset shows the far-infrared vibrational spectrum at 300 K. (b) Two functions, $(\alpha E)^2$ and $(\alpha E)^{1/2}$, useful for extracting direct and indirect gap information, as a function of photon energy at 5 (blue) and 300 K (red). Dashed lines guide the eye. Orange squares mark direct gap intercepts, whereas the green triangle marks the indirect gap intercept.

6 eV, which is due to transitions from the O 2p derived bands to the metal e_g bands. This correspondence means that the band positions are accurately determined by the LDA calculations. Based on our electronic structure calculations and comparison with previous studies,[5,15,17,18] we assign the feature centered at ~2 eV to a Rh^{3+} d → d (t_{2g} to e_g) on-site

(12) Mattheiss, L. F. *Phys. Rev. B* **1991**, *43*, 1863.
(13) Singh, D. J.; Blaha, P.; Schwarz, K.; Mazin, I. I. *Phys. Rev. B* **1999**, *60*, 16359.
(14) Singh, D. J.; Gupta, M.; Gupta, R. *Phys. Rev. B* **2001**, *63*, 205102.
(15) Ohta, H.; Nomura, K.; Hiramatsu, H.; Ueda, K.; Kamiya, T.; Hirano, M.; Hosono, H. *Solid-State Electron.* **2003**, *47*, 2261.

(16) With appropriate broadening this structure would likely correspond to the local minimum in the optical conductivity near 5 eV.

excitation. This symmetry forbidden transition is made possible due to crystal-field splitting of the Rh 4d orbitals and the hybridization of Rh d and O p states. Similarly, electronic excitations above 3 eV are assigned as O 2p → Rh 4d charge-transfer excitations.

The theory of energy gap determination from optical absorption spectra of solids is well-established. The absorption coefficient, $\alpha(E)$, consists of contributions from both the direct and the indirect band gap transitions[19] and is given by

$$\alpha(E) = \frac{A}{E}(E - E_{g,dir})^{1/2} + \frac{B}{E}(E - E_{g,ind} \mp E_{ph})^2, \quad (1)$$

where $E_{g,dir}$ and $E_{g,ind}$ are the magnitude of direct and indirect gaps, respectively, E_{ph} is the emitted (absorbed) phonon energy, and A and B are constants. The precise profile (eq 1) assumes a simple band shape and may not be exactly followed in a material with complex band structure. The direct energy gap can be extracted by plotting $(\alpha E)^2$ as a function of photon energy (E). The fit for a direct gap of $ZnRh_2O_4$, obtained from a linear extrapolation of $(\alpha E)^2$ to zero (as indicated by the dashed lines in Figure 5b), would be ~1.74 ± 0.02 eV at 300 K and ~1.79 ± 0.02 eV at 5 K. The gap sharpens at low temperature, a characteristic response. To extract the indirect gap parameters, it is usual to plot $(\alpha E)^{1/2}$ as a function of energy, as shown in Figure 5b. Two different slopes indicate the indirect nature of the absorption process.[19] The indirect energy gap and the phonon energy are estimated by extrapolating $(\alpha E)^{1/2}$ to zero, as indicated by the dashed lines. In particular, extrapolation of the two different slopes of $(\alpha E)^{1/2}$ shown to zero yields 1.21 and 1.46 eV. Within the model, these are $E_g - E_{ph}$ and $E_g + E_{ph}$, where E_{ph} is the phonon energy. Thus at 300 K, we find $E_g \sim 1.33 \pm 0.03$ eV, as indicated by the green triangle in Figure 5b. However, the phonon frequency is significantly above the calculated Raman frequency and the bond stretching infrared active phonon frequencies, as mentioned below. In a complex material like $ZnRh_2O_4$ several phonons could contribute to phonon assisted optical absorption, and so the effective frequency and precise shape of the spectrum may not be given by the simple expression above. This is true even in a structurally simple material such as GaN.[20] However, for single phonon processes the E_{ph} defining the onset cannot be higher than the maximum available phonon energy. Furthermore, the conductivity shows a similar 1.21 eV onset even at low temperature where there should be no significant phonon assisted absorption. Thus the value $E_g =$ 1.33 eV should be viewed as an upper bound on the gap, and considering the shape of the spectrum as compared with the calculated low-energy LDA spectrum, which does not include phonon assisted absorption, an alternate interpretation would be that the onset of absorption at 1.21 eV corresponds to the direct gap and the higher result of the direct gap fit (1.79 eV) corresponds to the onset of transitions to the flat bands at the top of the e_g manifold. Thus, the gap may be present only as a tail in the $(\alpha E)^2$ response (Figure 5b).

Interestingly, these values of the band gap are similar to those obtained in the trivalent compound Rh_2O_3.[21] However, as mentioned, there is no evidence for this phase in our sample. The single effective phonon energy parameter for the fit is ~125 ± 25 meV (1008 ± 200 cm^{-1}). The phonons coupled to the indirect transition can be optical or acoustic modes, depending on the material,[19,7,22] and here apparently high frequency optical phonons are involved. In an oxide, modes in this frequency range are generally bond stretching oxygen modes. These would be expected to modulate the metal−O hybridization, which would couple strongly to the optical response because the d−d transition is only allowed at lowest order due to the hybridization with O p states.

We measured the vibrational properties of $ZnRh_2O_4$ to check for evidence of the participating phonon mode in the indirect transitions (inset of Figure 5a). We observed four infrared active modes at 21.45 meV (173 cm^{-1}), 36.82 meV (297 cm^{-1}), 67.20 meV (542 cm^{-1}), and 73.52 meV (593 cm^{-1}), consistent with the group theory analysis for a spinel structure.[23] Based on vibrational properties studies in similar spinels,[23−26] we assign the vibrational modes at 73.52 and 36.82 meV to the asymmetric Zn−O stretching and bending modes in the ZnO_4 tetrahedra and the vibrational modes at 67.20 and 21.45 meV to the asymmetric Rh−O stretching and bending modes in the RhO_6 octahedra. From our estimate of the indirect gap and phonon energy required to activate the excitation, we find that at least two vibrational modes are coupled to the indirect gap excitation. Based upon energy scale arguments, the participating modes are likely the 67.20 meV (542 cm^{-1}) and 73.52 meV (593 cm^{-1}) Rh−O and Zn−O stretching modes, respectively.

IV. Conclusions

Based on our optical measurements and comparison with density functional calculations, we conclude that the band gap of spinel $ZnRh_2O_4$ is ~1.2 eV, which is much lower than previously reported. With the exception of the value of the band gap, we do find that the scenario for a good photoelectrode material is satisfied in this material. The band gap is small, even though the conduction band is high enough above the O 2p states to be above the H^+/H_2 potential. The correspondence between experimental measurements and the calculated band structure supports the view that density functional calculations can be used to calculate band gaps in this type of material, in agreement with the argument of Mattheiss.[12] Optical spectroscopy is very useful for this

(17) Narushima, S.; Mizoguchi, H.; Shimizu, K.; Ueda, K.; Ohta, H.; Hirano, M.; Kamiya, T.; Hosono, H. *Adv. Mater.* **2003**, *15*, 1409.
(18) Kamiya, T.; Narushima, S.; Mizoguchi, H.; Shimizu, K.; Ueda, K.; Ohta, H.; Hirano, M.; Hosono, H. *Adv. Funct. Mater.* **2005**, *15*, 968.
(19) Pankove, J. I. *Optical Processes in Semiconductors*; Dover Publications: New York, 1971.
(20) Reynolds, D. C.; Look, D. C.; Jogai, B.; Molnar, R. J. *Solid State Commun.* **1998**, *108*, 49.
(21) Koffyberg, F. P. *J. Phys. Chem. Solids* **1992**, *53*, 1285.
(22) Macfarlane, G. G.; McLean, T. P.; Quarrington, J. E.; Roberts, V. *Phys. Rev. B* **1958**, *111*, 1245.
(23) White, W. B.; DeAngelis, B. A. *Spectrochim. Acta, Part A* **1967**, *23*, 985.
(24) Shaplygin, I. S.; Lazarev, V. B. *Russ. J. Inorg. Chem.* **1980**, *25*, 504.
(25) Grimes, N. W. *Spectrochim. Acta, Part A* **1972**, *28*, 2217.
(26) Julien, C. M.; Massot, M. *Mater. Sci. Eng., B* **2003**, *97*, 217.

benchmarking. Finding an effective material based on $ZnRh_2O_4$ for electrochemical decomposition of H_2O would depend on chemical modifications that either increase the crystal field splitting or narrow the t_{2g} and/or e_g manifolds to produce a larger band gap.

Acknowledgment. We are grateful for helpful discussions with L. A. Boatner, F. M. Brown, and I. Paulauskas. Research sponsored by the Division of Materials Science and Engineering, Office of Basic Energy Sciences, U.S. Department of Energy, under Contract DE-AC05-00OR22725 with Oak Ridge National Laboratory, managed and operated by UT-Batelle, LLC. Work at the University of Tennessee was supported by the Materials Science Division, Office of Basic Energy Sciences, U.S. Department of Energy (DE-FG02-01ER45885).

CM060160V